E. Atlee Jackson, Phys. Rev. 153, 230 (1967); N. Tzoar, *ibid.* 164, 518 (1967); 165, 511 (1968); K. Nishikawa, J. Phys. Soc. Japan 24, 916 (1968); 24, 1152 (1968); A. F. Bakai, Zh. Eksperim. i Teor. Fiz. 55, 266 (1968) [Sov. Phys. JETP 28, 40 (1969)]; J. R. Sanmartin, Phys. Fluids 13, 1533 (1970); D. K. Kaw, E. Valeo, and J. M. Dawson, Phys. Rev. Letters 25, 430 (1970); S. M. Krizoruchko, A. F. Bakai, and E. A. Kornilov, Zh. Eksperim. i Teor. Fiz. Pis'ma v Redaktsiyu 13, 369 (1971) [JETP Letters 13, 262 (1971)].

[2]R. A. Stern and N. Tzoar, Phys. Rev. Letters 17, 903 (1966); R. A. Stern, *ibid.* 22, 767 (1969); M. Porholab and R. P. Chang, *ibid.* 22, 826 (1969); S. Tanaka, R. Sugaya, and K. Mizuno, Phys. Letters 28A, 650 (1969); G. Laval, R. Pellat, and M. Perulli, Plasma Phys. 11, 579 (1969); R. A. Stern, in *Proceedings of the Tenth International Conference on Phenomena in Ionized Gases* (Oxford U. P., 1971), p. 319; A. Y. Wong and R. J. Taylor, Phys. Rev. Letters 27, 644 (1971); A. F. Bakai, Zh. Eksperim. i Teor. Fiz. 59, 116 (1970) [Sov. Phys. JETP 32, 66 (1971)]; Y. Amagishi, K. Yamagina, H. Kozima, and K. Kato, Phys. Letters 36A, 241 (1971).

[3]E. Atlee Jackson, in Ref. 1.

[4]J. I. Gersten and N. Tzoar, Phys. Rev. Letters 27, 1650 (1971). The theory in that letter was presented in kinetic-theory language, but the physics is perhaps more transparent in a hydrodynamic formalism.

[5]E. O. Kane, J. Phys. Chem. Solids 1, 249 (1957); C. K. N. Patel, R. E. Slusher, and P. A. Fleury, Phys. Rev. Letters 17, 1011 (1966); P. A. Wolff and G. A. Pearson, *ibid.* 17, 1015 (1966); N. Tzoar and J. I. Gersten, *ibid.* 26, 1634 (1971); Phys. Rev. B 4, 3540 (1971).

[6]See N. Tzoar and J. I. Gersten, in Ref. 5.

[7]C. Hilsum and A. C. Rose, *Semiconducting III-V Compounds* (Pergamon, New York, 1961); *Semiconductors and Semimetals*, edited by R. K. Willardson and A. C. Beer (Academic, New York, 1966).

[8]Betsy Ancker-Johnson, in Ref. 7, Vol. I.

PHYSICAL REVIEW B VOLUME 6, NUMBER 4 15 AUGUST 1972

Lattice Location by Channeling Angular Distributions: Bi Implanted in Si

S. T. Picraux*
Sandia Laboratories, Albuquerque, New Mexico 87115

and

W. L. Brown and W. M. Gibson
Bell Telephone Laboratories, Murray Hill, New Jersey 07971

(Received 10 February 1972)

Measurements of 1-MeV He^+ channeling have been used to study the lattice location of ion-implanted Bi in Si. Single-alignment ⟨110⟩ and ⟨111⟩ angular distributions for He scattering from both the Si and Bi atoms at the same depth were measured as a function of implant conditions at 296 and 80 K. Double-alignment angular distributions were also measured for uniaxial and 90° biaxial channeling along ⟨110⟩ axes. For both single- and double-alignment measurements, the widths of the Bi distributions show significant narrowing relative to those for Si. Also, the Bi minimum yield is reduced from 16% for ⟨110⟩ single alignment to 5% for ⟨110⟩ uniaxial double alignment. Angular-distribution calculations based on the average-potential model were made for single-alignment axial channeling as a function of equilibrium displacement of an atom from a substitutional lattice site. The best agreement with the data is obtained for the case of ≈50% of the Bi displaced 0.45 Å from Si lattice sites and the remaining Bi atoms located substitutionally on Si lattice sites.

I. INTRODUCTION

An important technique for directly determining the lattice location of impurities in single crystals is the use of energetic-particle channeling. For example, when the reductions in the backscattering yield for various crystal channeling directions are the same for the impurity as for the lattice atoms, then the impurity atoms are determined to be on substitutional lattice sites. For cases where part or all of the impurity atoms occupy nonsubstitutional sites the interpretation is less straightforward. A minimum requirement for the unambiguous assignment of lattice locations seems to be careful angular scans along various channeling directions for both the impurity and the lattice atoms. In principle, the fact that the beam flux density varies across the channel region between the lattice rows or planes[1] should allow the technique to be sensitive to any well-defined location within the unit cell. However, an understanding of the ultimate experimental limitations of the technique is still needed.

Most channeling studies have been performed in a single-alignment rather than double-alignment mode. For single-alignment channeling measure-

ments the ion beam is incident along a crystal axis or plane and ions are detected which exit the crystal along a nonchanneling direction, whereas for double alignment the ions both enter and exit along channeling directions. The double-alignment technique has been used primarily to enhance the sensitivity of the channeling effect to impurity atoms or defects. However, since the flux distribution of the ion beam across the channel is not uniform, double-alignment measurements, as indicated in the present work, give valuable additional information for lattice-location studies.

Examples of recent progress in lattice-location studies by single-alignment measurements include the study of interstitials in Si[1,2] and W[3] for which peaking in the angular distributions is observed. This effect is due to the increased beam flux density in the center of the channel.[4-6] A second important result has been the determination of the sublattice occupied by a substitutional species in a diatomic lattice.[7] Bi was found to occupy P sites in GaP by comparing the Bi angular distribution for the ⟨110⟩ direction to that for pure-Ga and pure-P rows.

Another class of problems is that of impurity atoms only slightly displaced from lattice rows. Earlier measurements[8,9] of angular distributions have shown a narrowing of the impurity distribution (channeling dip) relative to that for the lattice atoms for Bi and Sb implanted in Si. The largest effect was seen for the Bi dips. It has been suggested that this may be due to the impurity atoms being displaced 0.1–0.2 Å from the Si lattice rows.[9,10]

A closely related area involving small displacements from the lattice rows is the study of nuclear lifetimes. The observed blocking dip from the emission of a reaction product depends on the distribution of recoil distances of the compound nucleus from the crystal row or plane. Recent angular-distribution calculations[11,12] for these systems, however, are not directly applicable to the case of equilibrium displacements since they involve a distribution of displacements dependent on the decay process.

In this study we have extended the lattice-location studies for the case of Bi in Si using single-alignment channeling measurements of the angular distributions. In addition uniaxial and biaxial double-alignment channeling distributions were measured. To our knowledge double-alignment distributions have not previously been measured. Channeling calculations of the single-alignment angular distributions based on the average-potential model[13] also were made for atoms as a function of displacement distance for the lattice row. Comparisons of calculations with measurements indicate certain general features and suggest a possible semiquantitative model for the Bi location.

II. EXPERIMENTAL PROCEDURE

Samples were prepared from 1000-Ω cm p-type float-zoned silicon by bismuth implantation on a heavy-ion accelerator at Bell Telephone Laboratories (BTL). For single-alignment channeling measurements the Si was cut perpendicular to the (110) plane with the surface normal bisecting the angle between the ⟨111⟩ and ⟨110⟩ axes. This allowed comparison of channeling measurements along these two major axes with the beam direction at the same angle to the surface normal (≈18°) so that the Bi was at the same relative depth. For double-alignment channeling measurements a sample was cut on the (100) face so that two perpendicular ⟨110⟩ axes were at 45° to the surface normal.

Typical Bi implantations were at 150 keV, with fluences of $2-4\times10^{14}$ cm^2 at room temperature or above, along nonchanneling directions. For room-temperature implants the lattice disorder was annealed in flowing dry N_2 for 30 min at 650 C.

Channeling-effect measurements were carried out by monitoring the large-angle scattering of a 1-MeV He^+ beam as a function of crystal orientation. The beam diameter was 1 mm with full angle divergence less than 0.06°. The sample was oriented by a two-axis goniometer which could be set reproducibly to 0.01° and maintained at room temperature (≈296 K) or at 80 K. Measurements were made in a turbo-pumped chamber at $\lesssim10^{-6}$ Torr. A secondary electron shield biased to −200 V surrounded the sample, which was in turn surrounded by a liquid-nitrogen shield to reduce surface contamination.

For single-alignment measurements an Au surface-barrier Si annular detector was placed collinear with the beam with a full-acceptance angle of 18°. The backscattered He ions were energy analyzed with a resolution full width at half-maximum (FWHM) ≈20 keV. The total Bi yield was integrated together for the angular-distribution measurements, where the projected range and the standard deviation in the projected range for 150-keV Bi in Si are 515 and 125 Å, respectively.[14] The Si yield was measured over a constant energy interval at energies corresponding to the *same* average depth as the implanted Bi so that the relative Si and Bi angular distributions may be directly compared without significant depth corrections.[15] All yields are normalized by the yield for a nonchanneling direction. Tilts through ⟨110⟩ and ⟨111⟩ axes were made at an angle of 16.8° with respect to the {110} plane. The He^+ fluence was increased in the region of the minimum to maintain a total

Bi yield of 400–1200 counts (typical Si yield was 10 000 counts) and the beam current was varied to limit the counting rate dead time to < 3%. Typical measurement currents were 1 nA and maximum fluences for angular positions near the axis were 1 μC for single alignment. The currents and fluences for double alignment were approximately a factor of 100 higher. The influence of the He analyzing beam was examined by measurements of the Bi minimum yield as a function of He fluence along a nonchanneling direction. Only a small effect was observed with the yield increasing from $\approx$9% initially to a constant level $\approx$14% after 8-μC fluence for fluences up to 540 μC.

Two simultaneous double-alignment channeling measurements were performed with two detectors, a cooled annular detector along the beam direction for uniaxial channeling (full-acceptance angle $\approx 0.38°$) and a collimated detector at 90° to the beam direction for biaxial channeling (full-acceptance angle $\approx 0.14°$). Both uniaxial and biaxial detectors had translational position control with respect to the sample direction. Thus, after using the goniometer to align a ⟨110⟩ crystal axis with the incident-beam direction, the biaxial detector was translated to a position to detect particles exciting the crystal along the ⟨110⟩ axis at 90° to the beam direction. In making the angular scan for the double-alignment measurements each point was taken at a new position on the sample to reduce any radiation-damage effects due to the He^+ beam, since high fluences are required to obtain adequate statistics. This was accomplished by translating the biaxial and uniaxial detectors and by "dog-leg" electrostatic steering of the beam to maintain a parallel beam direction during translation. The number of Bi atoms/cm^2 was determined independently by backscattering measurements along nonchanneling directions at each position on the sample to normalize for effects of lateral nonuniformities of the Bi implantation on the double-alignment yields.

III. EXPERIMENTAL RESULTS

A. Single-Alignment Channeling

The ⟨110⟩ axis angular distributions for Bi in Si are shown in Fig. 1 for 1-MeV He^+ channeling at 296 K. The Si sample was implanted with 150-keV Bi at room temperature to a fluence of 1.8×10^{14}/cm^2 and then annealed for $\frac{1}{2}$ h at 650 C. No significant change in the distribution was observed after an additional anneal at 840 C. Similar angular distributions were observed for a 150-keV implant at 450 C and a 40-keV implant at 350 C for 2.4×10^{14} Bi atoms/cm^2. In the region of the shoulders of the dip (1°–3°) the Si and Bi distributions are similar. However, at smaller angles the Bi dip is significantly narrower than that for the Si lattice and the minimum yield is greater. Single-alignment channeling measurements were also made for the ⟨111⟩ axial distribution at 296 K on the same sample. As shown in Fig. 2, the results were similar to the ⟨110⟩ dips with slightly more narrowing of the entire Bi dip. The measurements shown in Figs. 1 and 2 were repeated for the sample temperature at 80 K. As shown in Figs. 3 and 4 for the ⟨110⟩ and ⟨111⟩ axes, respectively, the Bi dip is again significantly narrower than that for the Si, particularly

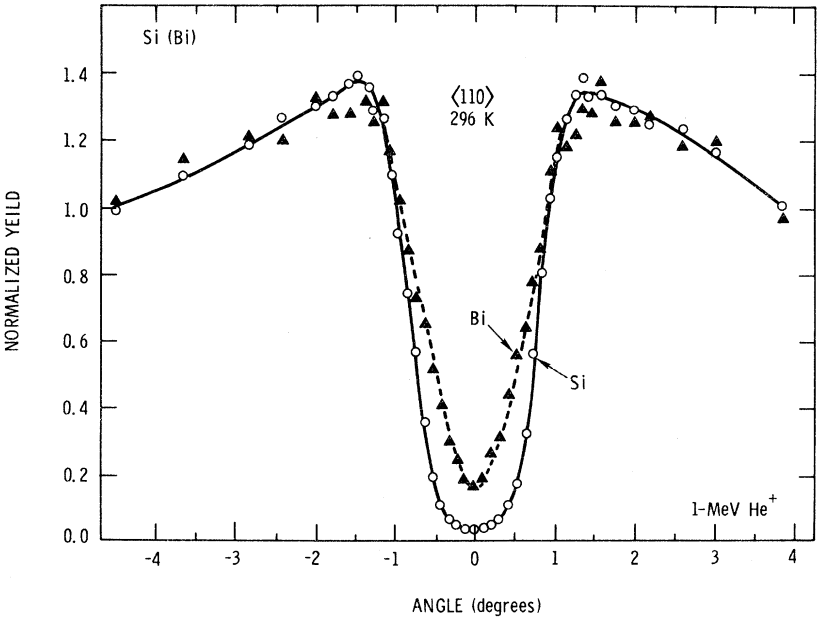

FIG. 1. Single-alignment channeling angular distributions for 1-MeV He^+ scattering from Bi (triangle) and Si (circle) for a Bi-implanted Si sample. Measurements are for the ⟨110⟩ axis at 296 K.

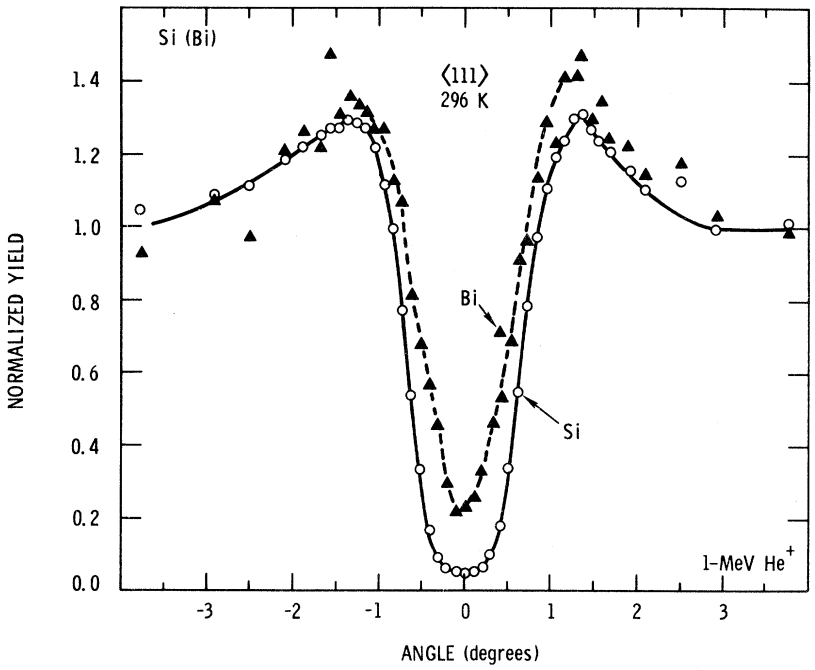

FIG. 2. Channeling distributions as in Fig. 1 for the ⟨111⟩ axis at 296 K.

in the lower part of the dip. Some differences are also observed between the Bi and Si shoulders for the ⟨110⟩ 80-K results.

A simple way to characterize the angular distributions is to specify the critical angle $\psi_{1/2}$ and the minimum yield χ. The critical angle is the half-width of the dip at a level halfway between the minimum yield and the yield for a nonchanneling direction; whereas χ is the ratio of the yield for the beam incident parallel to the channeling direction to the yield for a nonchanneling direction. Our measured $\psi_{1/2}$ and χ values for the Si and Bi angular distributions are given in Table I.

The single-alignment dips (Figs. 1–4) all show the same general decrease in slope for the sides of the Bi dip relative to that for Si. Also, there is some indication of an inflection point for several of the Bi curves in the region of 0.4 to 0.7 relative yield. These results suggest that the Bi atoms are not all located substitutionally on Si lattice sites, as might be expected for a group-V dopant.

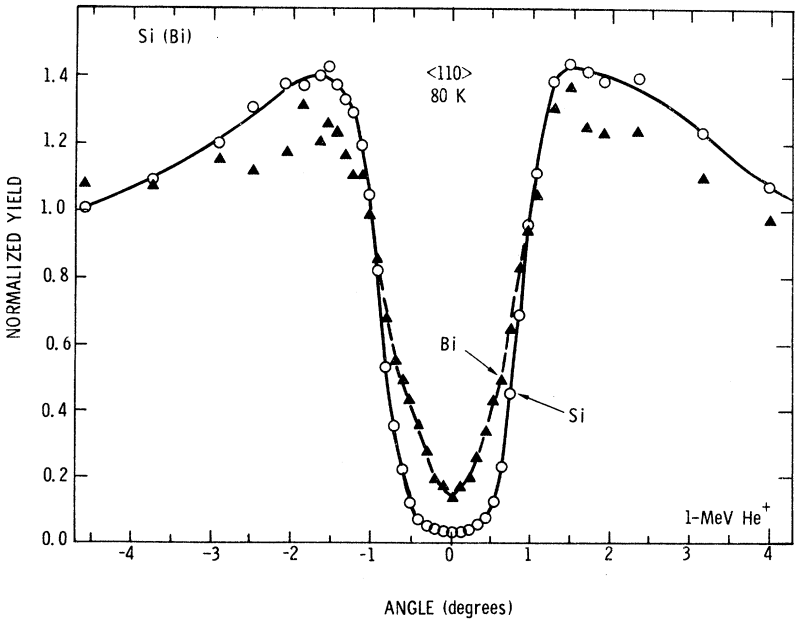

FIG. 3. Channeling distributions as in Fig. 1 for the ⟨110⟩ axis at 80 K.

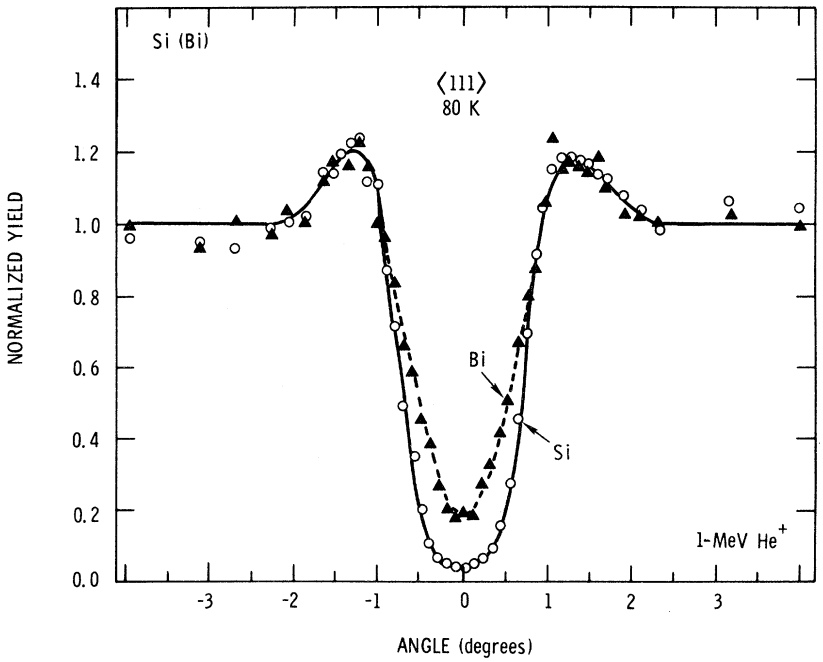

FIG. 4. Channeling distributions as in Fig. 1 for the ⟨111⟩ axis at 80 K.

Previous measurements[16] of the Bi minimum yields along the ⟨111⟩ and ⟨110⟩ axes suggested that approximately 85% of the Bi atoms were on lattice sites and the other 15% were off lattice sites (for example, at precipitation sites). Our minimum yields are in agreement with these earlier measurements; however, the narrow angular distributions suggest that the Bi atoms may have an equilibrium position slightly displaced from substitutional sites with more than 85% of the Bi *near* lattice rows.

B. Double-Alignment Channeling

Double-alignment measurements were made to gain more information about the location of the Bi atoms. The results of [110] uniaxial (channeling in and out along the same axis) and 90° biaxial (channeling in along the [110] axis and out along the [$\bar{1}$10] axis) distribution measurements are shown in Fig. 5. The measurements were made using 1-MeV He^+ at 296 K for a room-temperature 150-keV 2×10^{14} Bi atoms/cm^2 implant annealed to 650 C for $\frac{1}{2}$ h. The measured critical angles and minimum yields are given in Table II. The Bi dips are again narrower relative to the Si dips (Fig. 5) but tend to show the same relative narrowing at the top and bottom of the dips, in contrast to the single-alignment results. The ⟨110⟩ Bi minimum yield is reduced significantly from $\approx$0.15 for single alignment to $\approx$0.05 for double alignment, as shown in Fig. 6. This suggests that at least 95% of the Bi atoms are near lattice rows.

For atoms on lattice rows, calculations[17,18] of the minimum yields for double alignment χ' have indicated $\chi' = \nu(\alpha)\,\chi^2$, where χ is the single-alignment yield and $\nu(\alpha)$ is a constant of the order of 1 to 2, dependent on the angle α between the incoming and outgoing channeling axes. Therefore, for Bi atoms near lattice rows where the flux density is less than 1, the double-alignment yield should be further reduced approximately as the square of the flux density. The measured double-alignment

TABLE I. Single-alignment critical angles[a] and minimum yields[a] for Si implanted with Bi.[b]

Implant temp. (°C)	Anneal temp. (°C)	Analysis temp. (°C)	Axis	$\psi_{1/2}$(deg) Si	$\psi_{1/2}$(deg) Bi	χ Si	χ Bi
23	650	−193	⟨110⟩	0.79	0.69	0.035	0.15
		−193	⟨111⟩	0.70	0.61	0.049	0.18
		23	⟨110⟩	0.71	0.57	0.039	0.16
		23	⟨111⟩	0.61	0.47	0.051	0.23
23	840	23	⟨110⟩	0.75	0.64	0.049	0.20
450	none	23	⟨110⟩	0.72	0.60	0.040	0.19

[a]Measured at a depth in silicon corresponding to the depth of the Bi implant.

[b]All implants at 150 keV to fluences $2\text{–}4\times10^{14}$/cm^2.

TABLE II. Double-alignment critical angles and minimum yields for Si implanted with Bi.

	Axes	α	$\psi_{1/2}$ (deg) Si	$\psi_{1/2}$ (deg) Bi	χ' Si	χ' Bi
Biaxial	[110]·[$\bar{1}$10]	90°	0.90	0.70	0.0033	0.040
Uniaxial	[110]·[110]	180°	0.91	0.68	0.0059	0.050

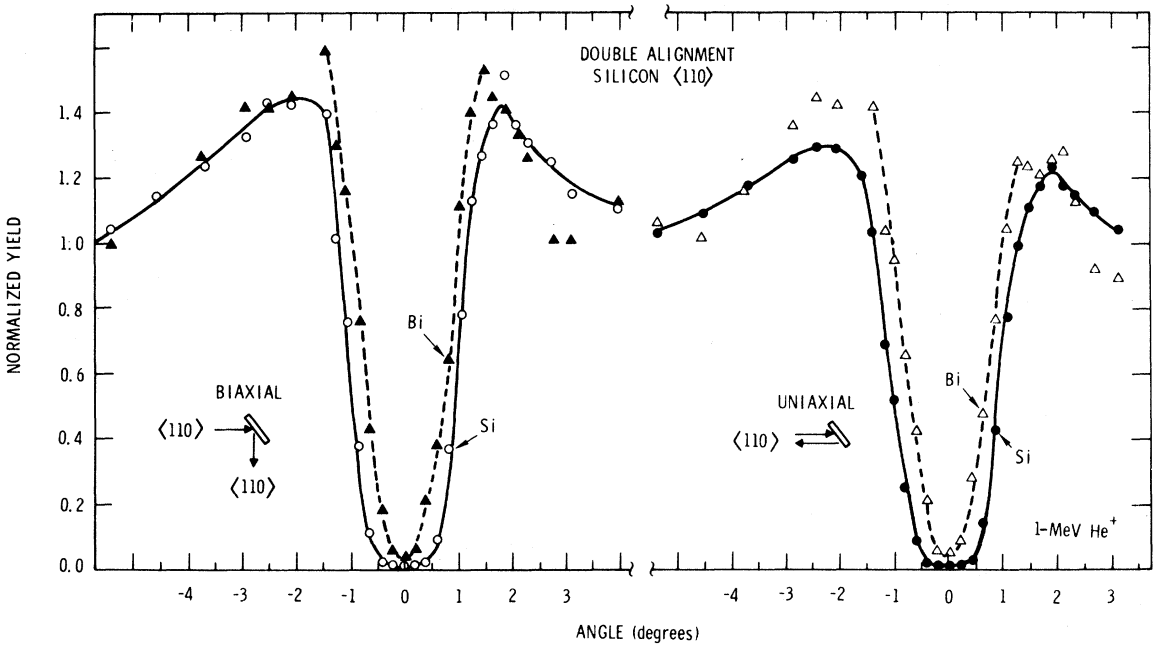

FIG. 5. Uniaxial and 90° biaxial double-alignment angular distributions for ⟨110⟩ axes. Bi and Si dips for 1-MeV He^+ scattering from a Bi-implanted Si sample.

and single-alignment minimum yields are compared for both the Si and Bi scattering in Table III. The ν values for the Si lattice are about a factor of 2 to 3 larger than those expected theoretically for a perfect crystal and are comparable to measurements by Appleton and Feldman[17] for pure Ge crystals. The ν values for Bi are approximately equal to the calculated values for lattice atoms. The reason for the larger ν value for Si than for Bi may be the residual implantation disorder remaining after the 650 C anneal or dischanneling by a surface oxide layer. Because of the much lower

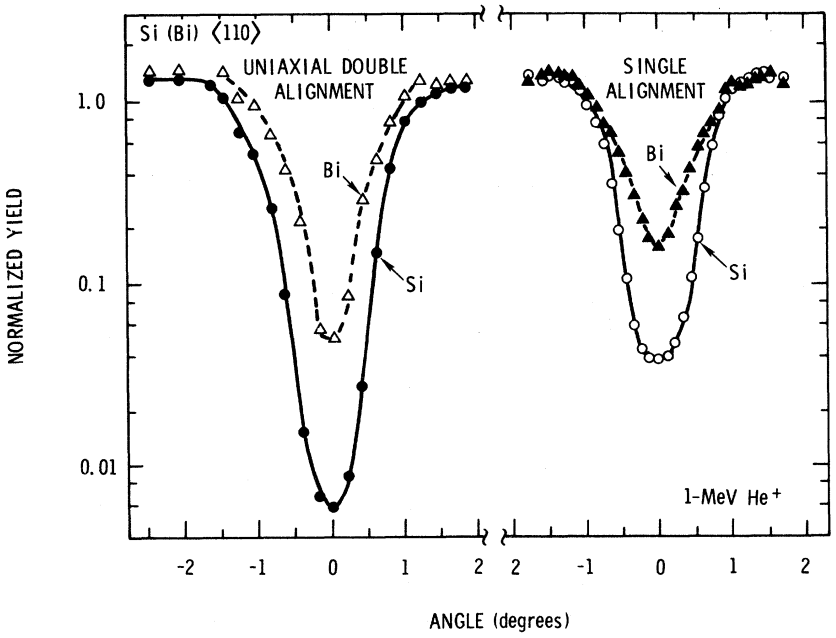

FIG. 6. Comparison on semi-log scale of single and uniaxial double-alignment ⟨110⟩ angular distributions in Figs. 1 and 5.

TABLE III. Comparison of single- and double-alignment minimum yields.

	α	χ	χ'	(χ'/χ^2)
Si	90°	0.039	0.0033	2.17
	180°	0.039	0.0059	3.88
Bi	90°	0.164	0.040	1.49
	180°	0.164	0.050	1.86

scattering yield from the Si than the Bi, the Si is much more sensitive to any such contributions.

IV. CALCULATION

The experimental differences between the Si and Bi channeling angular distributions have suggested[9,10] that the Bi atoms may be displaced from substitutional Si lattice sites. In order to gain more information about the Bi location we have calculated the angular distributions for single-alignment axial channeling as a function of the *equilibrium displacement* of an atom from a lattice row. The calculation is based on the average-potential model developed by Lindhard.[13] This model has been quite successful in predicting the relative angular widths over a wide range of crystal targets and incident-ion parameters.[19,20] Similar calculations for *substitutional* atoms have been carried out previously by Andersen using the halfway-plane approach.[20] In detail, a vibrating lattice atom is considered to be emitting particles isotropically, and the distribution in transverse energy of the particles with respect to the atom row is calculated at a plane halfway between the atoms in the row. Changes in the transverse energy distribution of the particles during passage through the crystal are neglected, and the angular distribution of the particles (blocking pattern) outside the crystal is obtained by accounting for the surface transmission. This angular distribution may be directly related to the probability of an ion hitting an atom as a function of incident-ion beam angle with respect to the crystal row (i.e., channeling angular distribution).

The coordinates for the emission of a particle are illustrated by Fig. 7. The position of the emitting atom in the x-y plane with respect to the distance from the row of atoms (z axis) is described in terms of a Gaussian probability distribution about the equilibrium position. In cylindrical coordinates we have

$$dP(r',\theta') = \alpha' \exp\left[-\left(\frac{r'}{\rho}\right)^2 - \left(\frac{x_0}{\rho}\right)^2 + \frac{2x_0 r' \cos\theta}{\rho^2}\right] \frac{d(r'^2)}{\rho^2}\, d\theta' , \quad (1)$$

where x_0 is the equilibrium displacement distance from the row, ρ^2 is the mean-square vibrational amplitude in the plane perpendicular to the row about the equilibrium position, and α' is a normalization constant dependent on x_0/ρ. The emission from the atom at a position (r', θ') is described by spherical coordinates (φ, θ) at that position with the z' axis parallel to the atom row (z axis). The transverse energy of the emitted particle is defined as the sum of the kinetic and potential terms by

$$E_\perp = E\varphi^2 + U(r_1) , \quad (2)$$

where E is the energy of the emitted particle and U is the average potential of the row of atoms. We have used Lindhard's standard potential and have neglected the vibrations of the atoms in the row. However, the calculation can be carried out equally well for other potential approximations and for thermal averaging of the potential. The value r_1 in Eq. (2) is the perpendicular distance of the emitted particle from the row after it has traveled a distance $\frac{1}{2}d$ in the z direction where d is the average spacing of atoms along the row. As seen in Fig. 7, r_1 is determined by variables $(x_0, r', \theta', \varphi, \theta)$ from the set of equations

$$r_1^2 = r^{*2} + x_0^2 - 2r^* x_0 \cos\gamma ,$$

$$r^{*2} = r^2 + (\tfrac{1}{2}\varphi d)^2 + r\varphi d \cos\theta ,$$

$$r^2 = r'^2 + x_0^2 - 2r' x_0 \cos\theta' ,$$

$$\cos\gamma = \left(\frac{[r^2 + r^{*2} - (\tfrac{1}{2}\varphi d)^2]\,(r^2 + x_0^2 - r'^2)}{4r^2 r^* x_0}\right)$$

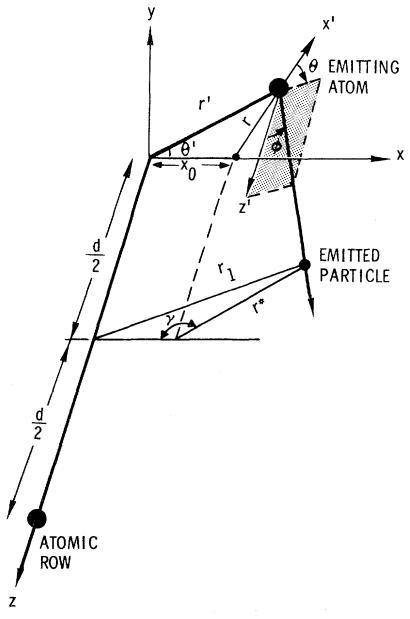

FIG. 7. Geometry for channeling-angular-distribution calculation.

$$-(\tfrac{1}{2}\varphi d)\left(\frac{r'}{rr^*}\right)\sin\theta\,\sin\theta'. \quad (3)$$

The transverse energy distribution in the crystal is then given by

$$\Pi(E_\perp)=\int_{r'=0}^{r_0}\int_0^{2\pi} dP(r',\theta')\int d(E\varphi^2) \times\int_0^{2\pi}\frac{d\theta}{2\pi}\,\delta(E_\perp - U(r_1) - E\varphi^2), \quad (4)$$

where the average area occupied by each row is $\pi r_0^2=(Nd)^{-1}$ for N the atomic density. The distribution in angle ψ_e of the emitted particles with respect to the row after transmission through the surface as given by Andersen[20] is

$$P_e(E\psi_e^2)=\int_0^{r_0}\frac{d(r^2)}{r_0^2-\hat{r}^2\,[E\psi_e^2+U(r)]}\,\Pi[E\psi_e^2+U(r)], \quad (5)$$

where $\hat{r}[E\psi_e^2+U(r)]$ is defined by $U(\hat{r})=E\psi_e^2+U(r)$. The normalized yield P_e as a function of angle ψ_e is obtained by numerical integration of Eqs. (4) and (5) following Andersen's procedure,[20] except that $\hat{r}$ has not been set equal to zero. The distributions have been normalized to one at an angle ψ_e equal to five times the characteristic angle for channeling.

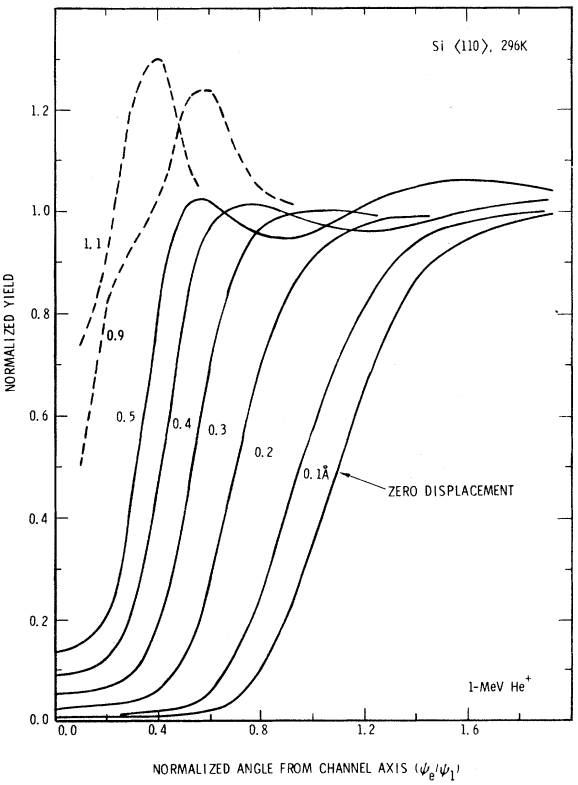

FIG. 8. Calculated single-alignment angular distributions as a function of equilibrium displacement distance from the row in Å for 1-MeV He^+ along the ⟨110⟩ axis in Si at 296 K.

Results of 1-MeV He^+ calculations for the ⟨110⟩ row in Si at 296 K are shown in Fig. 8 as a function of displacement distance x_0 from the ⟨110⟩ row. Using the measured Si Debye temperature[21] $\Theta_D=543$ K, we have $\rho=0.106$ Å, while r_0 and d are 1.26 and 3.84 Å, respectively. Angles in Fig. 8 are normalized to the characteristic angle for channeling $\psi_1=(2Z_1Z_2e^2/Ed)^{1/2}$, where Z_1 and Z_2 are the atomic numbers of the emitted particle and the lattice atoms, respectively. The angular width of the channeling dip is seen to decrease rapidly with increasing displacement from the lattice row, and the minimum yield increases. Qualitatively similar behavior to that shown in Fig. 8 was found for calculations of 1-MeV He^+ on the Si⟨111⟩ axis at 296 K and for the ⟨110⟩ and ⟨111⟩ axes at 80 K.

In the calculation we have neglected the adjacent rows and assumed a cylindrically symmetric potential. This approximation, as well as that of an average potential, becomes increasingly less accurate with increasing displacement distance. However, we have indicated by dashed lines calculated results for $x_0=0.9$ and 1.1 Å. These results qualitatively show the transition to flux peaking, where in the limit of an atom in the center of a channel there is a relative probability significantly greater than unity of being hit by a channeled ion than by an unchanneled ion.

Calculations have also been made for equilibrium displacements up to 0.5 Å along the z direction by letting $(\frac{1}{2}d)\rightarrow(\frac{1}{2}d\pm z_0)$. For the average potential treatment the changes in z have negligible effect on the angular distribution relative to the x_0 contribution. Therefore, in the comparisons with experimental data only the component of the displacement perpendicular to the row is considered. A Monte-Carlo-type binary-collision calculation[18,22] could be used to extend the studies to large displacements perpendicular to the row and even to include the effects of relaxation in the position of neighboring atoms along the row. However, agreement between binary-collision and average-potential models for substitutional lattice atoms suggests that reasonable agreement may be obtained by our average-potential calculation for small displacements from the lattice row, particularly with respect to the shape of the sides of the distribution.[23]

The case of an isotropic Gaussian distribution of displacements about a substitutional lattice site can be simulated by increasing the root-mean-square vibrational amplitude ρ. The results for up to four times the value of ρ at 296 K are shown in Fig. 9. There is a uniform narrowing of the dip and an increase in minimum yield

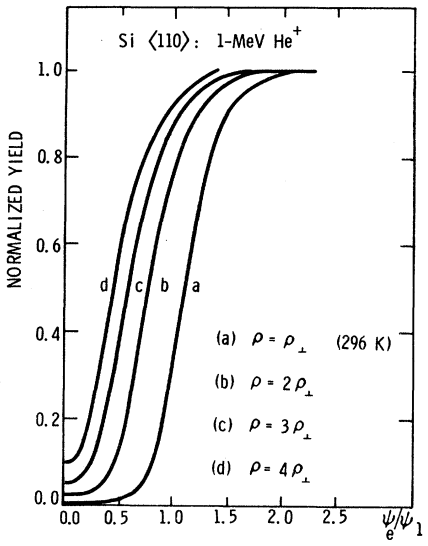

FIG. 9. Calculated ⟨110⟩ angular distributions for 1-MeV He^+ incident on Si for atoms on lattice sites as a function of atom vibrational amplitude. $\rho_\perp = 0.106$ Å is the root-mean-square value transverse to the row for Si at 296 K.

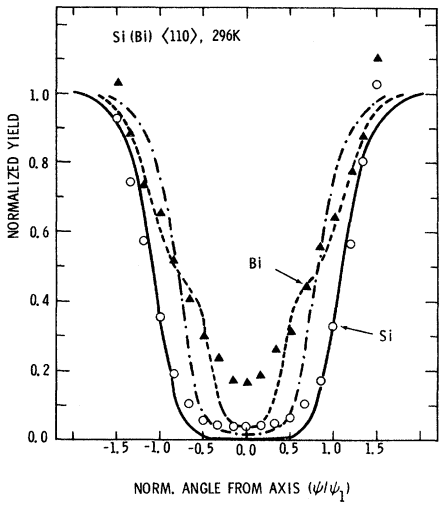

FIG. 10. Comparison of angular-distribution calculations with measurements (see Fig. 1) for the ⟨110⟩ axis at 296 K where the solid line is for Si, the dot-dashed line is for Bi assuming all of the Bi atoms displaced 0.2 Å along the ⟨110⟩ directions, and the dashed line is for 50% of the Bi displaced 0.45 Å along the ⟨110⟩ directions and 50% on substitutional lattice sites.

qualitatively similar to that for a uniform displacement in Fig. 8.

V. COMPARISON OF MEASUREMENTS AND CALCULATIONS

A. Si Angular Distributions

Comparisons between the calculated and measured dips for the Si lattice as a function of lattice row and temperature are shown in Figs. 10–13. The solid lines represent the calculation and the open circles give the measured Si points taken from Figs. 1–4. The experimentally measured angle ψ is normalized by ψ_1 and related to the calculated value ψ_e/ψ_1 by a constant, $\psi/\psi_1 = b(\psi_e/\psi_1)$. The need for a factor b arises from depth effects[15] which are neglected in the calculation and from deficiencies in a single-string model.[18,23] The value of $b = 0.75$ was determined by fitting the width of the 296-K ⟨110⟩ Si dip to the measurements, and this same value was used for all the Si and Bi curves.

The agreement of calculation and experiment in the width and slope of the sides of the Si dips is good, even though the measured widths vary significantly with direction and temperature (see Table I). The agreement is less satisfactory in the region of the minimum of the dip, where the observed yield is significantly greater than the calculated level. The calculated minimum yield in the curves corresponds to that obtained by the simple-average-potential-theory estimate[13] $\chi = N\pi d\rho^2$. Barrett[18] has shown by Monte Carlo calculations that a better estimate is given by $3N\pi d\rho^2$. In addition, we estimate from the Si surface peak of the ⟨110⟩ spectrum that the surface is covered by approximately 85 Å of oxide which gives an additive contribution[13] to the ⟨110⟩ minimum yield $\chi_3 \approx 0.015$. Thus, using a more realistic estimate given by $\chi \approx 3\chi_{\text{calc}} + \chi_3$, where $\chi_{\text{calc}} \approx N\pi d\rho^2$ for the Si dips, we obtain 0.034 and 0.043 for the ⟨110⟩ and ⟨111⟩ minimum yields, respectively,

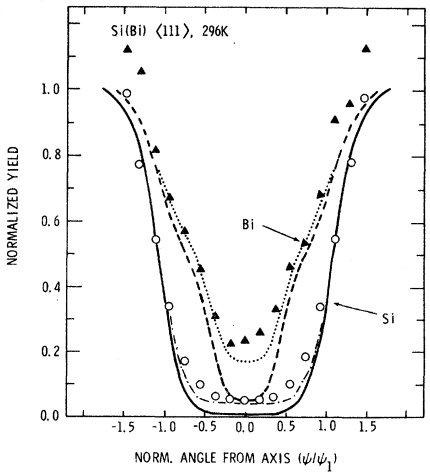

FIG. 11. As in Fig. 10 for the ⟨111⟩ axis at 296 K where the solid line is for Si and the dashed curve for Bi with the same location as for the dashed curve of Fig. 10. The dot-dashed and the dotted curves include calculated minimum-yield corrections to the Si (solid) and Bi (dashed) curves, respectively.

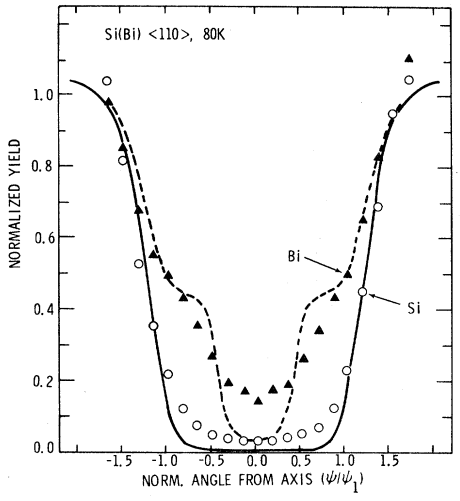

FIG. 12. As in Fig. 10 for the ⟨110⟩ axis at 80 K.

which is in better agreement with the observed values 0.039 and 0.051 (see Table I). This estimate is still slightly low, probably due to residual lattice disorder remaining after the anneal of the Bi implant.[24] We also note that the calculated dips do not predict the high yields in the shoulders of the distribution; these are primarily due to "planar effects" which depend on the tilt orientation and are not accounted for in the axial dip calculation.[25]

B. Bi Angular Distributions

The agreement of the width and the shape of the sides for the Si dips between measured and calculated values suggests that qualitative agreement might similarly be expected for the Bi dips for calculations using the correct Bi location. To compare the calculations for a displaced atom with respect to a given row to the measured results in Si, one must include symmetry considerations of all the possible displacements which occur due to the six equivalent ⟨110⟩ rows and four equivalent ⟨111⟩ rows. We have assumed that a Bi displacement in a particular crystal direction with respect to a given row (e.g., [110]) will have an equal probability of displacement to equivalent sites with respect to the other rows (e.g., [$\bar{1}$10], [101], [$\bar{1}$01], [011], [0$\bar{1}$1]). Since the channeling measurement is made along a particular row, the calculated angular distributions must be averaged together to correspond to the perpendicular displacements from that row for the equivalent sites with respect to the other rows. Although we do not have a detailed knowledge of the vibrational nature of Bi in the Si lattice, large-amplitude resonances are not expected since the Bi mass is much heavier than that for Si. Therefore the mean-square vibrational amplitude of Bi has been assumed to be the same as that of the Si lattice atoms in all the calculations.[26]

In order to calculate the Bi angular distribution we must specify the Bi site(s) and the fractional amount of Bi atoms on each site. We specify the Bi site by a vector from a Si lattice site of magnitude and crystal direction corresponding to the Bi displacement. Our approach is to begin with the simplest possible assumptions concerning the Bi location and examine which of these gives angular distributions consistent with our experimental results.

Since assuming all the Bi are on Si lattice sites clearly does not give agreement with the Bi data (solid Si lines in Figs. 10–13), we begin in accordance with previous suggestions[9,10] by assuming that all the Bi atoms have an equilibrium displacement a small distance δ from Si lattice sites. The result of a displacement $\delta = 0.2$ Å along the ⟨110⟩ direction is shown in Fig. 10 by the dot-dashed line for the room-temperature ⟨110⟩ Bi dip. Choosing instead a displacement in the direction of the Si tetrahedral interstitial site (along ⟨111⟩) gives the same result within the resolution of the drawing. In general we may say that while the critical angle can be accounted for by fixed displacement of all the Bi atoms, the qualitative agreement of the shape of the sides of the dip with our experimental Bi data (triangles in Fig. 10) is far from satisfactory.

The lack of agreement for a single displacement has led us to consider that the Bi may be distributed between two different equilibrium sites. We have therefore assumed that only a fraction of the Bi, f_D, has an equilibrium displacement and that the rest $(1 - f_D)$ are on Si lattice sites. The displaced fraction f_D and the displacement distance δ have been varied for several displacement direc-

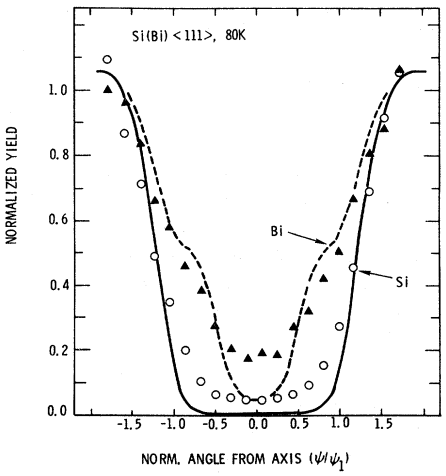

FIG. 13. As in Fig. 10 for the ⟨111⟩ axis at 80 K.

tions to give the best agreement with the four measured distributions for the ⟨110⟩ and ⟨111⟩ axes at 296 and 80 K. The results for 50% of the Bi atoms having a displacement $\delta = 0.45$ Å along the ⟨110⟩ axis with the other 50% on lattice sites are shown by the dashed lines of Figs. 10–13. The agreement with experiment (triangles) of the shape of the sides of the ⟨110⟩ dip at 296 K is seen to be quite reasonable (Fig. 10). As for the Si distributions, the calculated minimum yield is considerably lower than the measurements. Using this same Bi location the agreement of the shape of the sides of the dip is fair for the ⟨111⟩ dip at 296 K (Fig. 11) and somewhat poorer for 80-K measurements (Figs. 12 and 13). Changes in the displacement distance and/or fraction displaced in excess of 10–20% give noticeably poorer agreement with the 296-K measurements. The sensitivity to displacement direction is somewhat less, however. For example, calculations for the same displacement δ and displaced fraction f_D along the ⟨111⟩ direction give similar agreement, except in the case of the ⟨111⟩ dip at 296 K, where the calculated curve is noticeably wider. In general the displacement distance and fraction can be specified with greater confidence than the displacement direction.

The inflections in the sides of the calculated dips at 80 K (Figs. 12 and 13) would become less prominent if some relaxation of the equilibrium displacement distance occurred with decreasing temperature. Such a temperature dependence would not be unreasonable to expect and would give better qualitative agreement with both the width and shape of the 80-K dips. Also, the nuclear multiple scattering of the beam in traversing the 85 Å of surface oxide would tend to smooth any inflections in the observed angular distributions since the rms multiple scattering angle is calculated from theoretical estimates[13] to be $\approx 0.14°$.

The agreement between calculation and experiment in the regions of the Bi and Si minimum yields is not satisfactory and suggests the need for a better quantitative approach. If for comparison we consider the same modification to the Bi minimum yield as argued for the Si lattice, $\chi \approx 3\chi_{calc} + \chi_3$, we obtain for Bi $\chi \approx 0.15$ and 0.18 for the ⟨110⟩ and ⟨111⟩ at 296 K, respectively, which is in better agreement with the observed values of 0.16 and 0.23. We note that the factor of 3 was determined for atoms on lattice sites for $\psi = 0$ and may be somewhat different for displaced Bi atoms. However, the effect of this correction on the angular distributions can at least be indicated by an additive correction (with renormalization) to the calculated curves. This is shown in Fig. 11 for the 296-K ⟨111⟩ distributions by the dotted and dot-dashed line for Bi and Si, respectively. The greatly improved agreement with the measurements in Fig. 11 argues for the correctness of this modification for the region of the minimum yield.

Lattice strain from high concentrations of Bi atoms or lattice defects might result in a distribution of the Bi equilibrium position about Si lattice sites. The case of an isotropic Gaussian distribution can be simulated by increasing the effective mean-square vibrational amplitude of the emitting atom, as was shown in Fig. 9. This does not give good qualitative agreement with the observed results, but instead tends to give a uniform narrowing of the dip similar to the case of all the atoms being displaced a fixed amount.

Although it is straightforward to extend the model to more complex combinations of Bi displacements, such elaboration does not seem justified without first improving the calculation. Angular distributions obtained by Monte Carlo computer simulations would be a valuable complement to these studies.

VI. DISCUSSION

In these channeling-effect studies of impurity-atom location we have tried in a semiquantitative way to make use of the entire angular distribution for the impurity-atom scattering rather than just the minimum yield and angular width. Several important features have emerged from the single-alignment studies. The special lattice-location behavior of Bi implanted in Si appears to be independent of the implantation conditions. Both hot and annealed room-temperature implants give rise to the same narrowing of the Bi channeling dip. In addition to the fluences used in these measurements (≈ 2–$4 \times 10^{14}/\text{cm}^2$), the narrowing of the dip has also been observed previously by blocking patterns in α-emission studies[27] for fluences $\approx 10^{13}$ cm^2. The possibility that the He$^+$ analyzing beam may affect the Bi location cannot be eliminated, but the small effects ($\lesssim 5\%$) observed for heavy He bombardments do not suggest a strong radiation sensitivity.[28]

Comparisons of calculated single-alignment angular distributions with our measurements suggest that it may not be possible to account for the Bi location by a single displacement of all the Bi atoms. Better agreement is obtained by a two-component model where part of the Bi is assumed to be displaced and the remainder to be on latti sites. Although unambiguous assignment of the Bi location cannot yet be given, a best fit to our data is obtained by assuming that $\approx 50\%$ of the Bi are displaced 0.45 Å from Si lattice sites and 50% are located substitutionally on Si lattice sites.

Important additional information is contained in double-alignment channeling distributions. The additional drop in the Bi minimum yield from $\approx 16\%$ for single alignment to $\approx 5\%$ indicates (accord-

ing to flux-distribution arguments) that at least 95% of the Bi are near lattice rows ($\lesssim 0.6$ Å). Also, the relation between the Bi double- and single-alignment yields $\chi' \cong \nu\chi^2$ as shown in Table III is not inconsistent with previous arguments indicating $\nu \approx 2$. The increase in angular width for double alignment over that for single alignment, as indicated by $\psi_{1/2}$ values in Tables I and II, may partially be explained by the lower energy of the scattered He ions and the $E^{-1/2}$ dependence of the angular width for blocking. The relatively greater $\psi_{1/2}$ increase for Si ($\approx$25%) compared to that for Bi ($\approx$15%) is consistent with the smaller fractional energy remaining upon He scattering from Si (0.563 for $\theta = 180°$) than from Bi (0.926 for $\theta = 180°$). However, to more fully utilize the data double-alignment angular-distribution calculations are needed as well as a more quantitative treatment of both single- and double-alignment distributions in the region of the minimum yield. For example, it is important to try to understand the qualitative difference in the shape of the Bi dip for single- and double-alignment measurements. For double alignment the Bi dips show a fairly uniform narrowing relative to the Si, whereas for single alignment the Bi dips are narrower primarily near the bottom of the dip.

Finally, it is of interest to consider how the Bi lattice location suggested by these calculations might arise. The larger size of the Bi atom (atomic radius $r_a = 1.70$ Å) relative to the Si lattice atoms ($r_a = 1.32$ Å) may play an important role, perhaps by defect or impurity association to relieve strain fields. Under these conditions variations in the Bi locations with depth might be expected across the implanted region. A smaller but measurable narrowing of the channeling dip also has been observed for Sb ($r_a = 1.59$ Å) implanted in Si.[8,9] Also, the Bi concentrations in these implanted layers ($\bar{N}_{Bi} \approx 6\times 10^{19}/\text{cm}^3$ for 150-keV, 2×10^{14} Bi atoms/cm^2) are more than two orders of magnitude above the equilibrium solid solubility of Bi in Si. Since electrical measurements[29,30] have indicated that active concentrations well in excess of equilibrium-solid-solubility limits are achievable for group-V implants in Si, these high concentrations may play an important role in the Bi location. Recent electrical activity and Hall mobility measurements[30] for Bi-implanted Si gave electrically active fractions ≈ 0.6 and mobilities appreciably lower than those expected for bulk Si of comparable resistivities. These results are not inconsistent with the present lattice-location results. Other measurements of Bi-implanted Si which are sensitive to the Bi location (EPR, NMR) or Bi-associated energy levels (electrical, optical) could give important support to the understanding of the Bi location.

ACKNOWLEDGMENTS

Valuable discussions with J. U. Andersen, D. K. Brice, B. Domeij, J. A. Ellison, J. W. Mayer, and D. Sigurd and technical assistance by J. W. Rodgers and R. G. Swier are acknowledged. One of the authors (S.T.P.) would like to thank his coauthors for their kind hospitality during his visits at BTL.

---

*Work supported in part by the Atomic Energy Commission.

[1]J. U. Andersen, O. Andreasen, J. A. Davies, and E. Uggerhøj, Radiation Effects 7, 25 (1971).

[2]B. Domeij, G. Fladd, and N. G. E. Johansson, Radiation Effects 6, 155 (1970).

[3]J. U. Andersen, E. Laegsgaard, and L. C. Feldman, Radiation Effects 12, 219 (1972).

[4]R. B. Alexander, G. Dearnaley, D. V. Morgan, and J. M. Poate, Phys. Letters 32A, 365 (1970).

[5]R. B. Alexander, G. Dearnaley, D. V. Morgan, J. Poate, and D. Van Vliet, in *European Conference on Ion Implantation* (Peregrinus, Stevenage, England, 1970), p. 181.

[6]D. Van Vliet, Radiation Effects 10, 137 (1971).

[7]J. L. Merz, L. C. Feldman, D. W. Mingay, and W. M. Augustyniak, in *Proceedings of the Second International Conference on Ion Implantation in Semiconductors*, edited by I. Ruge and J. Graul (Springer-Verlag, New York, 1971), p. 182.

[8]J. U. Andersen and J. W. Mayer (unpublished); J. W. Mayer, in *Semiconductors*, edited by S. Namba (Nagai, Tokyo, 1972), p. 137.

[9]D. Sigurd and B. Domeij, Phys. Letters 36A, 81 (1971); Radiation Effects (to be published).

[10]J. A. Davies, *European Conference on Ion Implantation* (Peregrinus, Stevenage, England, 1970), p. 172.

[11]G. J. Clark, J. M. Poate, E. Fuschini, C. Marconi, I. G. Massa, A. Uguzzoni, and E. Verondini, Nucl. Phys. A173, 73 (1971).

[12]K. Komaki and F. Fujimoto, Phys. Status Solidi 2, 875 (1970).

[13]J. Lindhard, Kgl. Danske Videnskab. Selskab, Mat. Fys. Medd. 34, 14 (1965).

[14]D. K. Brice, Sandia Laboratories Research Report No. 71-0599, 1971 (unpublished).

[15]S. U. Campisano, G. Foti, F. Grasso, and E. Rimini, Phys. Letters 35A, 119 (1971).

[16]L. Eriksson, J. A. Davies, N. G. E. Johansson, and J. W. Mayer, J. Appl. Phys. 40, 842 (1969).

[17]B. R. Appleton and L. C. Feldman, in *Atomic Collision Phenomena in Solids*, edited by D. W. Palmer and P. D. Townsend (North-Holland, Amsterdam, 1970), p. 417.

[18]J. H. Barrett, Phys. Rev. B 3, 1527 (1971).

[19]S. T. Picraux, J. A. Davies, L. Eriksson, N. G. E. Johansson, and J. W. Mayer, Phys. Rev. 180, 873 (1969).

[20]J. U. Andersen, Kgl. Danske Videnskab. Selskab, Mat. Fys. Medd. 36, 7 (1967).

[21]B. W. Batterman and D. R. Chipman, Phys. Rev. 127, 690 (1962).
[22]L. C. Feldman, Ph. D. thesis (Rutgers University, 1966) (unpublished).
[23]J. U. Andersen and L. C. Feldman, Phys. Rev. B 1, 2063 (1970).
[24]S. M. Davidson and G. R. Booker, Radiation Effects 6, 33 (1970).
[25]S. T. Picraux and J. U. Andersen, Phys. Rev. 186, 267 (1969).
[26]If, for example, the vibrational amplitudes for displaced Bi atoms were assumed to be increased over that for Bi atoms on lattice sites, there would be a corresponding decrease in the displacement distances to obtain the observed results. However, unreasonably large vibrational amplitudes would be required to significantly affect the results we obtain.
[27]J. O. Andreason, Ph. D. thesis (Aarhus University, 1971) (unpublished).
[28]E. Rimini, J. Haskell, and J. W. Mayer, Appl. Phys. Letters 20, 237 (1972).
[29]R. Baron, G. A. Shifrin, O. J. Marsh, and J. W. Mayer, J. Appl. Phys. 40, 3702 (1969).
[30]B. L. Crowder, J. Electrochem. Soc. 118, 943 (1971).

PHYSICAL REVIEW B VOLUME 6, NUMBER 4 15 AUGUST 1972

Two-Electron Band-to-Band Transitions in Solids*

K. Betzler, T. Weller, and R. Conradt
Physikalisches Institut der Universität Stuttgart, D-7000 Stuttgart, Wiederholdstr 13, *Germany*
(Received 29 November 1971)

In highly excited Si and Ge there appears an emission band at about $h\nu = 2E_g$, which is explained by two-electron radiative transitions across the band gap. The dependence on energy, temperature, and excitation intensity is measured and compared with theoretical calculations. The weak temperature dependence, the quadratic dependence on the injection current, and the energy dependence agree with the theoretical consideration. A transition coefficient of about 10^{-61} cm^9 sec^{-1} is found, in agreement with a rough theoretical estimate. The line shape indicates that, at least at room temperature, the two-electron transitions are phonon assisted. This leads also to the conclusion that the Auger recombination in Si must be phonon assisted, in contradiction to former considerations.

GENERAL

In previous papers the appearance of radiative two-electron transitions across the band gap was established.[1,2] Emission bands were observed in Si and Ge at an energy of about $h\nu = 2E_g$. In this paper we report further experimental results and give a more detailed examination of this effect.

Radiative two-electron transitions are well known in atomic physics in absorption, for example, as preionization. Heisenberg[3] has pointed out that the change of the angular momentum of the single particles in an electric-dipole transition is in first approximation $\Delta l_1 = \pm 1$, $\Delta l_2 = \pm 2$ or 0. In every case, the total change of angular momentum is $\Delta L = \pm 1$, if spin-orbit coupling is neglected.

In contrast to the atomic situation, in a solid both electrons may have the same initial state and the same final state, since l is no longer a good quantum number. For example, in the octahedral group O, transitions from Γ_{15} and Γ_{25} to all states may occur. Therefore, transitions between valence band and conduction band may occur with twice the energy of the one-electron transiton. Because of the strong absorption due to one-electron transitions at the energy of twice the band gap, the expected transitions can only be observed in emission.

Since energy doubling may also occur due to nonlinear optical effects, a material with inversion symmetry has to be chosen. In this case, electric-dipole transitions are not possible at the Γ point of the Brillouin zone because of the parity selection rule. In the k space away from the Γ point this selection rule does not hold. Therefore, an indirect-gap material has to be used. An additional advantage of an indirect-gap material is that in these materials the one-electron transitions near the band gap are not possible without other perturbation because of the momentum conservation, whereas the two-electron transitions are allowed if both electrons have opposite momentum in the indirect extrema. From these points of view and from experimental considerations, we have chosen indirect-gap semiconductors with inversion symmetry, namely, Si and Ge.

The line shape of the expected emission spectrum is calculated under the following assumptions. Because of the small relative change of energy and momentum transfer over the whole linewidth, we have assumed the transition matrix elements to be constant, i.e., we have calculated the line shape